MATEC Web of Conferences **280**, 04012 (2019) https://doi.org/10.1051/matecconf/201928004012
ICSBE 2018

Durability of RC Beams Strengthened Using GFRP-Sheet due to Fatigue Loads

Arbain Tata[1,*], *Anthonius Frederik* Raffel[1], *Muhammad* Ihsan[2], and *Rudy* Djamaluddin[3]

[1]Khairun University, Assoc. Professor of Civil Engineering Department, 97716 Ternate, Indonesia
[2]Sekolah Tinggi Teknik Baramuli, Lecturer, 91214 Pinrang, Indonesia
[3]Hasanuddin University, Professor of Civil Engineering Department, 90245 Makassar, Indonesia

Abstract. This paper presented the results of an experimental study of the behaviour of flexural beams strengthened with the glass fiber reinforced polymer (GFRP-S). This research was carried out to determine the effect of fatigue loads on the flexural capacity of reinforced concrete beams. The specimens were rectangular with a dimension of 150 mm in width, 200 mm in height, and 3300 mm in length. Four distinct conditions had been applied to this experiment. For the initial condition, two beams were tested under monotonic loads (maximum load control) as a control beam (BN). Sinusoidal fatigue loads were applied to four specimens from 4 kN to 24 kN (BF). Our comparative results of the experiment had presented that the normal beams (BN) failed after 800,000 loads cycle, while, the reinforced beams with GFRP (BF) failed after 1,231,860 loads cycle. Based on our results, it can be stated generally that fatigue life of the reinforcement beams (BF) could increase to more than 100% compared to that of the normal beams (BN). The failure of the beams is probably caused by fatigue of the reinforcement bar and debonding of the GFRP-S, both are secondary failure mechanism of reinforced concrete beams.

1 Introduction

The use of fiber reinforced polymer (FRP) materials has become a common practice for the repair and strengthening of concrete structures and bridges. Due to the success of this technique, several researchers have also investigated the use of externally bonded FRP materials for the repair and strengthening of steel bridges and structures. A number of different approaches have been investigated to assess the effectiveness of using FRP materials for rehabilitation of steel bridge girders including the repairing of naturally deteriorated girders. Strengthening or stiffening of the reinforced concrete and the pre-stressed concrete structures may be required as a response to an increase in load requirements, usage alteration, degradation of structure, and complexity in design as well as construction defects [1][2].

FRP is material with several advantages such as having high tensile stress, being lightweight and corrosion resistant, hence it would not contribute additional weight to the structure [3][4]. Moreover, the application of this material is very simple when compared to

* Corresponding author: arbatata@yahoo.co.id

conventional materials for structural rehabilitation or repair and it is safe for the environment because it is chloride-resistant [5]. The FRP technology could increase the capacity of the flexural beam. Vast studies have been conducted which implemented and applied this material for repairing or improving bridge functionality. The most common fiber materials used in advance fiber reinforced polymer composites for structural application are glass fiber, aramid and carbon. Among the three FRP materials, glass fiber is the most affordable while carbon is the most expensive one. In between is aramid whose costs is equal to low-quality carbon fiber. In this paper, the fiber material in discussion where glass fiber (GFRP-S). Principally, bridge structures including bridge-girders receive repetitive load from traffic loads. Several types of research had proved that repetitive loads in a bridge structure could provoke bridge failure, even when the load level is far below the ultimate flexural capacity [6]. In this regard, it is still necessary to improve the durability of reinforced concrete beam strengthened by FRP due to fatigue load.

2 Methodology

2.1 Specimen

Concrete used in the research was normal concrete with a design compressive strength of *f'c=25 MPa*. Compressive and flexural strength were examined through cylindrical compressive strength test and flexural beam test. Concrete casting was conducted in compliance with the standard. Concrete dismantling was conducted on day 3 of concrete life. Curing was then applied by covering the specimens with wet sack up to 28 days. All reinforced concrete beam specimens were designed in accordance with the design standard [8]. Eight beams for the material test were made; four were for control test on static load (BNS1, BNS2, BFS1, BFS2) and the other 4 were for fatigue loads (BN1, BN2, BF1, BF2). Figure 1 shows the details of the prepared test beam. The concrete beam had a cross-sectional dimension of 100 mm x 120 mm with 3,300 mm length. The Beam was designed to have reinforcement with 2D14 as a tensile reinforcement. To prevent from sliding failure, reinforcement bar with a diameter of 6 mm was used as stirrups. In this research glass fiber based FRP material in the form of sheet was used. The GFRP sheet was applied to wrap the tested beam. The combined properties of glass fiber and epoxy resin would form the GFRP-S. Some technical properties of GFRP-S are shown in Table 1 while the properties of the epoxy resin used in this research are shown in Table 2.

Application of glass fiber sheet material as beam's reinforcement was conducted after concrete beam had reached 28 days. The application process for strengthening beam was with a procedure in accordance with the standard. Initially, the surface of a beam at the pull side was cleaned using a polishing technique. The glass fiber sheet was then cut out according to the desired size and coated with epoxy resin. Then, the glass fiber sheet was affixed into the surface of concrete after the surface had been coated with epoxy resin as well. After properly positioned, the sheet material was then sealed off and coated with epoxy resin using a roller that the entire sheet became saturated with epoxy material. Further, the test material was left dry to make the epoxy resin material harden and fused with the glass fiber material to form the GFRP-S attached to the bottom side of the reinforced concrete beam.

Table 1. Properties of GFRP-S type SHE-51A

Items	Properties
Modulus Young (GPa)	3.24
Tensile strength (GPa)	72.40
Strain Maximum (%)	4.5
Density (gr/cm^3)	2.55
Fiber thickness (mm)	0.36

Table 2 Properties of epoxy resin

Items	Properties
Tensile strength (MPa)	72.40
Modulus Young (GPa)	3.18
Bonding strength (MPa)	2.12

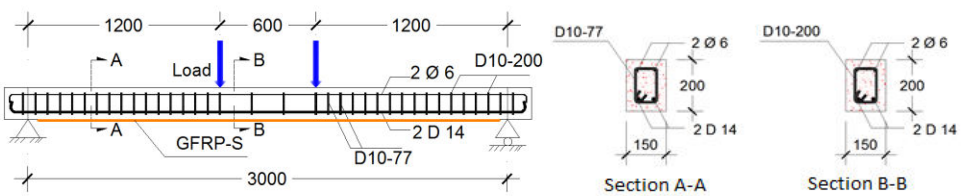

(a) Typical dimension of test specimens (b) Reinforcement details of test speciments

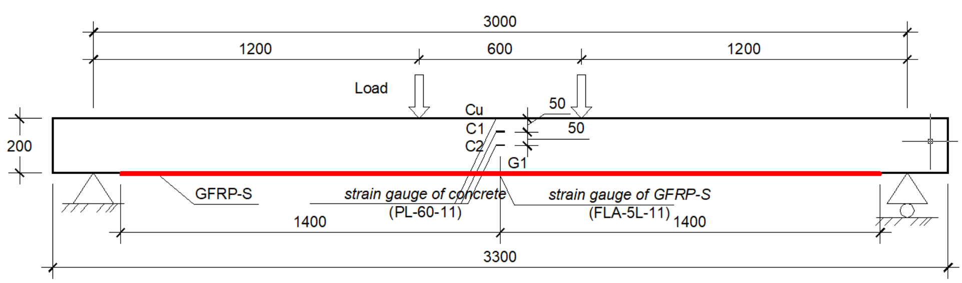

(c) Position of data recorder.

Fig. 1. Specimen details

Table 3. Summary of test specimens

Specimen Code	Specimens	Loading Type	Strengthening Schema
BNS	2	Static	Non GFRP
BFS	2	Static	With GFRP
BN	2	Fatigue	Non GFRP
BF	2	Fatigue	With GFRP

2.2 Testing method

Fatigue load was tested with fatigue testing instrument as shown in Fig. 1d with a loading capacity of 100 ton. Before the testing, strain gauges were affixed into the surface of the concrete and the surface of the GFPR-S to measure the strain in the test specimen during the loading process. Specimen beam was placed on top of two simple supports functioning as a placement system of joint. The load was given into two points at 50 cm distance at the middle of beam's span. The magnitude of load amount given was measured by using Load-Cell while the deflection was measured by using LDVT which was placed at the midpoint of the beam's span. All measurement instruments were connected into a data tabulation system and connected to the computer to monitor all measured parameters during the loading process. The beam was designed to be loaded by fatigue sine wave with minimum load 4kN (or around 5% from the ultimate flexural capacity) and maximum load 24 kN (or around 45% from the ultimate compressive strain of concrete). The minimum-maximum load pattern was given repeatedly with a frequency of 1.5Hz continuously until specimen failure. The data reading was conducted after the beam experienced repetitive load with a period of 10 cycles, 100 cycles and multiples of 50,000 cycles until beam failure. Determination of maximum-minimum load was based on the test result from the static load which was obtained from the observations of the relationship between load and strain occurring at the side of the maximum compressive side of the concrete.

3 Result and discussion

3.1 Effect of static load on the beam

Before further discussing the behaviour of the beam due to fatigue load, the discussion will then be about the behaviour of control beam due to monotonic load. This is intended to evaluate the influence of fatigue loads when compared with the influence of monotonic load. The stiffness of the structure is important. Stiffness restriction is used to keep the construction from yielding over the required deflection. Stiffness is defined as the force which is required to produce a unit of displacement. The value of stiffness is the angle of the slope of the relationship between load and deflection. According to Kenneth-Belanger (1981), the stiffness of a concrete beam is a function of the elastic modulus (E) and the moment of inertia (I). The inertia Ig denotes the inertia of beam which has not been cracked. Icr is used for inertia of beam after cracking, while the actual effective inertial moment value Ie is the value between Ig and Icr.

Table 4. Moment capacity from analysis and experiment.

Beam	Analysis				Experiment			
	P_y (kN)	M_y (kN.m)	P_U (kN)	M_U (kN.m)	P_y (kN)	M_y (kN.m)	P_U (kN)	M_U (kN.m)
BNS1	25.57	16.15	26.09	16.46	22.90	14.54	26.08	16.66
BNS2	25.57	16.15	26.09	16.46	22.80	14.50	26.44	16.84
BFS1	30.30	18.98	42.61	26.37	33.65	20.99	42.33	26.74
BFS2	30.30	18.98	42.61	26.37	32.31	20.24	43.73	27.02

In this research, there are 4 pieces of test beam loaded with monotonic load until the beam is cracked and destroyed immediately as the load increases. The four test objects are: BNS1, BNS2, BFS1, and BFS2 which can be seen in Fig. 2

Fig 2 depicts beam deflection behaviour for BNS1, BNS2, BFS1 and, BFS2. From the graph, it can be explained that the behaviours of each specimen are in accordance with the characteristics of each beam. For BNS1 beam, the loaded relationship at the beginning of loading is still a linear line showing full elastic behaviour up to 4.54 kN loading with a deflection of 2.07 mm. As the load increases, the reinforcing steel bar yields with a noticeably larger deflection without being followed by an increase in load with a load value of 24.57 kN and a deflection of 14.57 mm where the nonlinear load relation curve to deflection becomes much flatter than before. This occurs until the beam reaches a maximum load of 27.57 kN and deflection of 36.07 mm. As for BNK2 test specimen, the trend is still linear at the beginning of loading showing full elastic behaviour before reaching 4.07 kN load with a 1.62 mm deflection. As the load increases, the reinforcing steel bar starts to yield which is marked by a large increase in deflection without a significant load increase where the load value is 24.10 kN with a deflection of 14.21 mm, the nonlinear relationship curve is much flatter than before. This occurs until the beam reaches a maximum load of 25.70 kN and a deflection of 21.67 mm.

For BFS1 test object, the trend is still linear at the beginning of loading showing full elastic behaviour before reaching 10.88 kN load with a deflection of 3.88 mm. Increasing the load causes steel reinforcement to yield. A large increase in deflection without being followed by a significant load increase where the load value is 32.67 kN, with a deflection of 15.64 mm, the nonlinear relationship curve becomes much flatter than the previous stage. This occurs until the beam reaches a maximum load of 41.73 kN and deflection of 26.40 mm. On BFS2 test object, full elastic behaviour occurs before reaching 9.83 kN load with a deflection of 3.61 mm. As the load increases, the reinforcing steel undergoes a yield which is marked by a large increase in deflection without an increase in load which means the load value is 31.82 kN with a deflection of 15.52 mm, the relationship curve is much flatter than before. This occurs until the beam reaches a maximum load of 41.32 kN and a deflection of 27.29 mm.

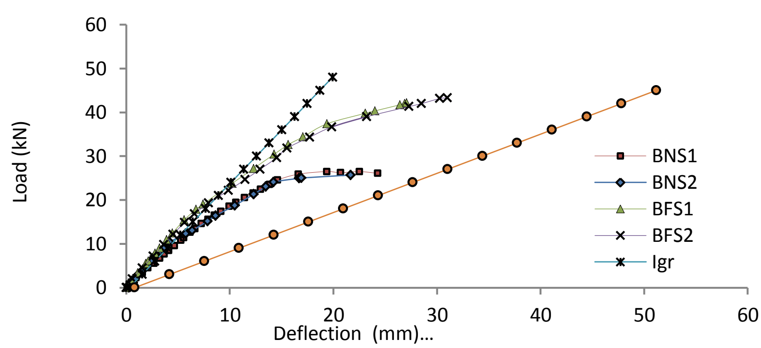

Fig. 2. Relationship of load to deflections of concrete beam BNS1, BNS2, BFS1 and, BFS2.

Ductility is the ability of structures or structural components to undergo repeated inelastic deformations after the initial yield, while maintaining sufficient strength and stiffness to support the load, so that the structure remains standing even when cracked and damaged. Ductility factor of building the structure the μ is the ratio of maximum deviation of the structure of building due to design earthquake effect near collapse condition Δu to the deviation of structure at the moment of initial yield Δy. In full elastic condition, μ value is equal to 1.0.

$$\boldsymbol{\varphi}_{\Delta} = \frac{\Delta_u}{\Delta_y} \tag{1}$$

The degree of ductility of the structure is influenced by the pattern of cracks or plastic joints, in which these plastic joints must be attempted to form at the ends of the beam and not on the supporting columns and walls. Mathematically, ductility is defined as the comparison of the displacement parameter of a structure at the time of collapse and displacement when the outer tensile reinforcement undergoes fatigue condition. The displacement ductility is the ratio of maximum structural displacement in the lateral direction to the displacement of the structure on yield phase [8].

From Table 5, it is obvious that there is a significant increase in the displacement ductility of reinforced concrete beam (BFS) at 14% than that of unreinforced concrete beam (BNS).

Table 5. Displacement ductility of beams

Description	**Experiment**				**DISPLACEMENT DUCTILITY**
	P*$_y$* **(kN)**	***Δ****$_y$* **(mm)**	***P****$_U$* **(kN)**	***Δ****$_u$* **(mm)**	***φΔ***
BNS1	25.57	15.49	26.08	38.92	2.51
BNS2	22.83	15.87	26.44	37.24	2.34
Average					**2.43**
BFS1	31.24	15.79	42.33	43.25	2.73
BFS2	33.65	15.92	43.73	44.56	2.79
Average					**2.77**

3.2 Effect of fatigue load on the beam deflection

Figure 5 shows the deflection on the normal beam for various loading levels after undergoing fatigue load cycle for up to 800,000 cycles of recurrent loads. At low loading level (P=4 kN), the deflection is still unnoticeable after fatigue loading. However, at a higher loading level, the effect of the repetitive loads has begun to be obvious. At 11.5 kN load, there is an increase in deflection after the beam experiences fatigue load of 800,000 cycles. At 19 kN load, the effect of fatigue load is more obvious where the deflection increases after loaded with 800,000 cycles of fatigue loads. The Guide for the Design and Construction of Externally Bonded FRP System for Strengthening Concrete Structure (ACI 440.2R-08). Notation Ms from Eq. (2) and (4) denotes moment due to all sustained loads plus the maximum moment induced in a fatigue loading tension condition on concrete that experiences bending as shown below in Fig. 3 and Fig. 4[7].

$$\boldsymbol{f_{s,s}} = \frac{\left[M_s+\varepsilon_{bi}A_f E_f\left(d_f-\frac{kd}{3}\right)\right](d-kd)E_s}{A_s E_s\left(d-\frac{kd}{3}\right)(d-kd)+A_f E_f\left(d_f-\frac{kd}{3}\right)(d_f-kd)} \tag{2}$$

$$\boldsymbol{f_{f,s}} = \boldsymbol{f_{s,s}}\left(\frac{E_f}{E_s}\right)\frac{((d_f-kd)}{(d-kd)} - \boldsymbol{\varepsilon_{bi}E_f} \tag{3}$$

$$\boldsymbol{M_s} = \frac{f_{s,s}(A_s E_s\left(d-\frac{kd}{3}\right)(d-kd)+A_f E_f\left(d_f-\frac{kd}{3}\right)(d_f-kd)}{(d_f-kd).Es} - \boldsymbol{\varepsilon_{bi}A_f E_f}\left(\boldsymbol{d_f}-\frac{kd}{3}\right) \tag{4}$$

Where $\boldsymbol{f_{s,s}}$ is stress level in non-prestressed steel reinforcement at service loads, $\boldsymbol{f_{f,s}}$ is stress level in FRP caused by a moment within elastic range of member, $\boldsymbol{M_s}$ is service moment at section, $\boldsymbol{E_f}$ is the tensile modulus of elasticity of GFRP-S, $\boldsymbol{E_s}$ is the modulus of elasticity of steel.

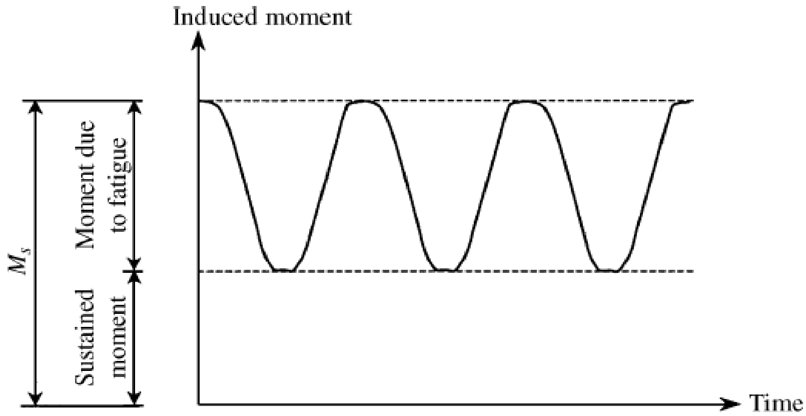

Fig.3. Illustration of the level of applied moment to be used to check the stress limits in the FRP reinforcement. (ACI Committee. 2008)

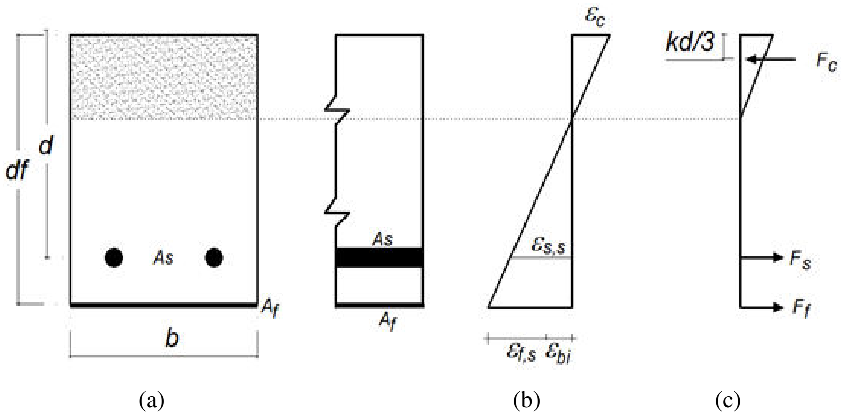

Fig.4. Internal strain and stress distribution for a rectangular section under flexural beams. (a) Reinforced concrete section, (b) Strain distribution, (c) Stress distribution

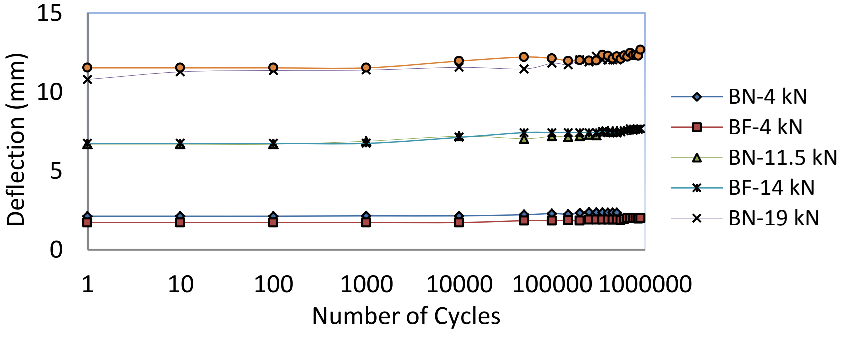

Fig. 5. Relationship of number of cycle and deflection on normal beam and GFRP beams.

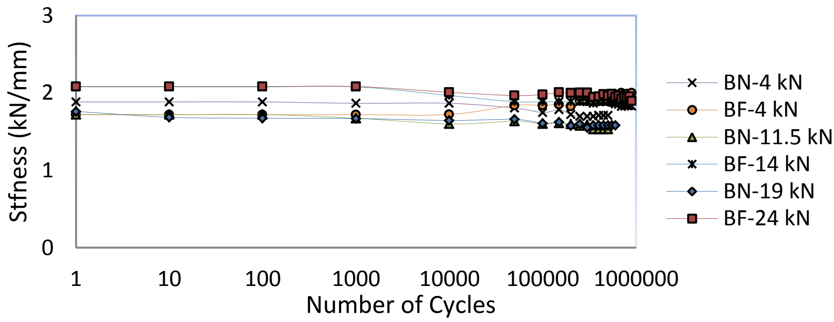

Fig. 6. Relationship of number of cycle and stiffness on normal beam and GFRP beams

Similarly, for beam reinforced by GFRP-S, the effect of fatigue load after 835,100 cycles for various loading levels causes an increase in the deflection to 17.73%, compared to the deflection on the beam loaded statically as shown in Table 6 and 7. The result shows that beams given with fatigue load 800,000 cycles tend to have greater deflection at the same loading level. This is caused by fatigue process either on concrete material or on reinforcing steel bar. The weakening at beam stiffness can be caused by a decrease in the adhesiveness between concrete reinforcing with concrete material and also the weakened between GFRP-S with the surface of the concrete. Generally, the weakening due to fatigue load is caused by the appearance of microcracks due to repeated loads.

Table 6. Comparison of beam deflection due to fatigue load and static load for normal beam

No	Active load (kN)	Deflection	
		Static load (mm)	Fatigue load (mm)
1	4.0	1.90	2.36
2	11.5	6.21	7.32
3	19.0	10.79	12.03

Table 7. Comparison of beam deflection due to fatigue load and static load for GFRP-S beam

No	Active load (kN)	Deflection	
		Static load (mm)	Fatigue load (mm)
1	4.0	1.72	2.06
2	14.0	6.74	7.52
3	24.0	11.53	12.24

3.3 Effect of fatigue load on concrete strain

Fig 7 shows the strain that occurs on the concrete's compressed side (outer compressed fiber) on the normal beam for various loading level after 835,100 cycles of fatigue load. At a relatively low loading level (P=4 kN), the strain is considered to change after fatigue load, but at a higher load level, it is shown that the effect of the fatigue loads has begun to emerge. At 11.5 kN load, there is an increase in strain after the beam experiences fatigue load of 800,000 cycles. At 19 kN load, the effect of fatigue load is more obvious where the strain experiences an increase after loaded with a fatigue load of 800,000 cycles. Phenomena in normal beam also occur in concrete beam reinforced by GFRP-S as shown in Fig. 7 which depicts the relation of strain to a number of cycles on a beam that strengthened by GFRP-S (BF) for various loading levels after passing fatigue loads of 1,231,860 cycles. At a relatively low load level (P=4 kN), the strain has not yet been affected by fatigue load. However, at a higher load level, the effects of repetitive load begin to appear. At 14 kN load, strain increases after beams experience fatigue loads of 1,231,860 cycles. At 24 kN load, the effect of fatigue loads is more obvious where the strain increases after loaded by fatigue loads of 1,231,860 cycles.

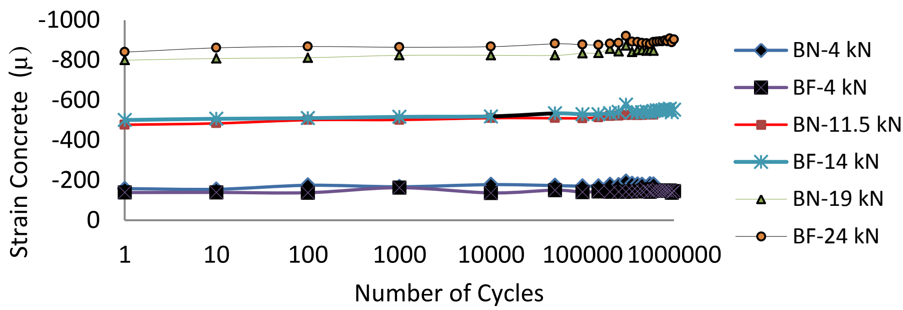

Fig. 7. Relation of concrete strain with total cycle for concrete reinforced by GFRP-S.

3.4 Collapse pattern after fatigue load cycles

Test beams were designed to undergo failure with under reinforcement failure pattern. The failure will be initiated with the reinforcement bar to yield following by concrete demolishing on the compressed side of the concrete. Based on beam static test, the maximum load for the normal beam is 24 kN and maximum load for the beam strengthened by GFRP-S is 42 kN. In the fatigue test, the maximum load is 19 kN for normal beam and maximum load for a beam with GFRP-S is 42 kN.

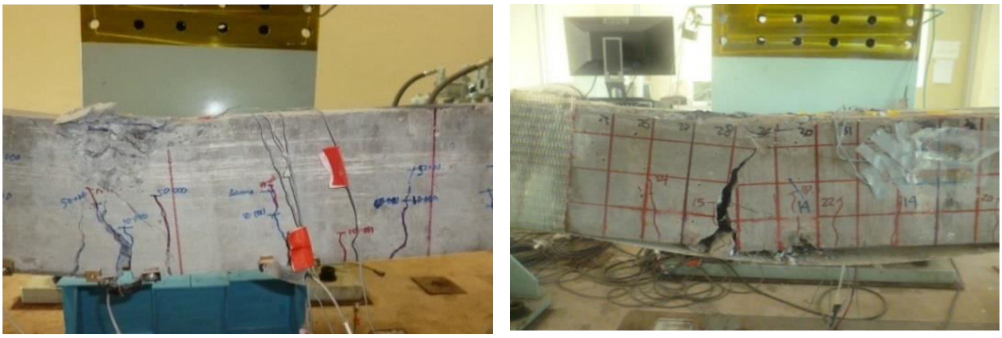

(a) (b)

Fig. 8. Failure pattern due to fatigue loading. (a) compressive failure of normal beam BN, (b) compressive failure on GFRP-S Beam (BF)

Although the maximum fatigue load is given only 60% from the ultimate beam load control, normal beam (BN) experiences blowing when loaded by 800,000 cycles of the load while for the reinforced beam (BF) the mechanism occurs after loaded by 1,231,860 cycles of the load. Figure 8 shows an image of beams experiencing failure after fatigue load. The failure of the beams is probably caused by the fatigue of the reinforcement bar and debonding of the GFRP-S, which is a secondary failure mechanism of reinforced concrete beams.

4 Conclusion

From the result and discussion of this research, the conclusion can be drawn as follows: Fatigue life has an effect on a deflection after loaded by fatigue load, which fails at 835,100 cycles (BN) and 1,231,860 cycles (BF). Due to fatigue load, beams tend to experience the stiffness weakening both on normal beam (BN) and GFRP-S reinforced beams (BF). Fatigue load has an effect on concrete compressive strain after loaded by fatigue load. Due to fatigue load, beams tend to experience an increase in the strain both on normal beam (BN) and GFRP-S reinforced beams (BF). Fatigue load can lead to beam failure even when the maximum load is still below the ultimate load the beam based on the static load. The beams fail primarily due to fatigue of the steel reinforcement. Debonding of the GFRP composite sheet a secondary mechanism in the strengthened beams.

References

1. C. Papakonstantinou, G, M. Petrou, F, K. Harries A., Fatigue Behavior of RC Beams Strengthened With GFRP-Sheet, J. of Composites for Construction, **5**, 4, pp.246-252 (2001).
2. A. Tata, R. Djamaluddin, H. Parung, W. Tjaronge., Ultimate Experiment of Ruptured Concrete Beams Strengthened Using GFRP-Sheet after Fatigue Loads, J. of Eng. and Tech., Constr. and Env. Eng. (IACSIT), **7**, 1, pp. 45-49 (2015).
3. S. Masoud, K. Soudki, T. Topper., CFRP-Strengthened and Corroded RC Beams Under Monotonic and Fatigue Loads, J. of Composites for Construction (ASCE), Vol.5; No. 4, pp. 0228-0236 (2002).
4. A. Vladimir, Volnyy, C. Pantelides P., Bond Length of CFRP Composite Attached to Precast Concrete Walls, Journal of Composites for Construction (ASCE), Vol. 3, No. 4, pp. 168 – 176 (1999).
5. A. Richard, Barnes, C. Geoffrey, Mays., Fatigue performance of Concrete Beams Strengthened with CFRP Plates, Journal of Composites for Construction (ASCE) Vol. 3. No. 2, Paper No. 18334 (1999).
6. M. Elkenel, J. John, F. Myers, ACE, Fatigue Performance of CFRP Strengthened RC Beams Under Environmental Conditioning and Sustained Load, Journal of Composites for Construction (ASCE), Vol. 13, No. 2, pp. 93-1002 (2009).
7. ACI Committee, ACI 440.2R-08: Guide for the Design and Construction of Externally Bonded FRP System for Strengthening Concrete Structures. USA, (2008).
8. P. Paulay, Priestley., Seismic Design of Reinforced Concrete and Masonry Buildings, John Wiley & Sons, New York (1992).